

# Hybridization-induced superconductivity from the electron repulsion on a tetramer lattice having a disconnected Fermi surface

Takashi Kimura<sup>1,2,3</sup>, Yuji Zenitani<sup>4</sup>, Kazuhiko Kuroki<sup>5</sup>, Ryotaro Arita<sup>1</sup>, and Hideo Aoki<sup>1</sup>

<sup>1</sup>*Department of Physics, University of Tokyo, Hongo, Tokyo 113-0033, Japan*

<sup>2</sup>*Graduate School of Frontier Sciences, University of Tokyo, Hongo, Tokyo 113-0033, Japan*

<sup>3</sup>*Advanced Research Institute for Science and Engineering, Waseda University, Tokyo 169-8555, Japan*

<sup>4</sup>*Department of Physics, Aoyama-Gakuin University, Chitosedai, Setagaya, Tokyo 157-8572, Japan*

<sup>5</sup>*Department of Applied Physics and Chemistry, University of Electro-Communications, Chofu, Tokyo 182-8585, Japan*  
(February 1, 2008)

Plaquette lattices with each unit cell containing multiple atoms are good candidates for disconnected Fermi surfaces, which are shown by Kuroki and Arita to be favorable for spin-fluctuation mediated superconductivity from electron repulsion. Here we find an interesting example in a tetramer lattice where the structure within each unit cell dominates the nodal structure of the gap function. We trace its reason to the way in which a Cooper pair is formed across the hybridized molecular orbitals, where we still end up with a  $T_c$  much higher than usual.

PACS numbers: 74.70.Kn, 74.20.Mn

The discovery of high- $T_c$  superconductors [1] has kicked off renewed interests in electronic mechanisms for superconductivity. In the course of studies it is becoming increasingly clear that superconductivity can arise from repulsive interaction between electrons. The essence there is electrons interact by exchanging spin fluctuations, which can effectively act as an attraction in the gap equation, if we consider anisotropic pairing with nodes in the gap function.

For the Hubbard model, this was first suggested from early calculations by Scalapino et al. [5]. Subsequently a quantum Monte Carlo calculation [6] indeed indicated an enhancement of the pairing correlation with  $d$ -wave symmetry in the repulsive Hubbard model. The superconducting critical temperature ( $T_c$ ) has been estimated with the fluctuation-exchange approximation (FLEX), a kind of renormalized random phase approximation. [2–4]

One remarkable point is  $T_c \sim O(0.01t)$ , estimated for the repulsive Hubbard model in the two-dimensional (2D) square lattice, is *two orders of magnitudes smaller than* the starting electronic energy (i.e., the hopping integral  $t$ ), although this gives the right order for the cuprates'  $T_c$ . Arita et al. then looked at various lattices (square, triangular, fcc, bcc, etc) in search of the most favorable case with a FLEX analysis [7]. The best case, as far as these ordinary lattices are concerned, turns out to be the 2D square lattice, so  $T_c < O(0.01t)$  remains. As discussed in Ref. [8], there are good reasons why  $T_c$  is so low, where an important one is the presence of nodes in the superconducting gap function greatly reduces  $T_c$ : While the main pair-scattering, across which the gap function has opposite signs to make the effective interaction attractive, some of the pair scatterings around the nodes have negative contributions to the effective attraction by connecting  $k$ -points on which the gap has the same sign.

So a next important avenue to explore is: can we

improve the situation by going over to multiband systems. Kuroki and Arita [8] have shown that this is indeed the case if we have *disconnected Fermi surfaces*. In this case  $T_c$  is dramatically enhanced, because the sign change in the gap function can avoid the Fermi pockets, where all the pair-scattering processes contribute positively. [8–10] This has been numerically shown to be the case for the triangular lattice (for spin-triplet pairing) [11] and a square lattice with a period-doubling [8], where  $T_c$  as estimated with FLEX is as high as  $O(0.1t)$ .

To be more precise, the key ingredients are: (a) when the Fermi surface is nested, the spin susceptibility  $\chi(\mathbf{q}, \omega)$  has a peak, with a width  $\Delta\mathbf{Q}$ . (b) When a multiband system with a disconnected Fermi surface has an inter-pocket nesting (i.e., strong inter-pocket pair scattering and weak intra-pocket one) the gap function has the same sign ( $s$ -wave symmetry) within each pocket, and the nodal lines can happily run in between the pockets.

Here a natural question is: to prepare multiband systems systematically, we can consider lattices comprising some units, or “plaquette lattices”. This is indeed considered by Kimura et al. [9] who conceived an idea of actually fabricating the structure from arrays of quantum dots. One example is the inset of Fig. 1, where the unit is a square lattice of squares, where the intra-plaquette transfer is stronger than the inter-plaquette one. Now, an important question is: how the structure of the superconducting gap function having higher  $T_c$ 's is determined and whether the  $s$ -wave symmetry on each pocket is compulsory.

In this paper, we study the repulsive Hubbard model on a square lattice of diamonds, where a diamond is a four-site unit rotated by 45 degrees (Fig. 1). One motivation is that this structure is reminiscent of the in-plane lattice of B and C in  $\text{CaB}_2\text{C}_2$  [12], so should not be too unrealistic, although we are not claiming to consider this

particular material. We have solved Eliashberg's equation [13] for the Hubbard model with the FLEX and obtained a  $T_c$  that is considerably higher than that of the square lattice. More importantly, however, the present model, despite of its disconnected Fermi surface, has sign changes in the gap function within each pocket, so a different mechanism should be at work. We can trace back its reason in *real space* that the singlet pairing here results from a hybridization of two *molecular orbitals* in each plaquette.

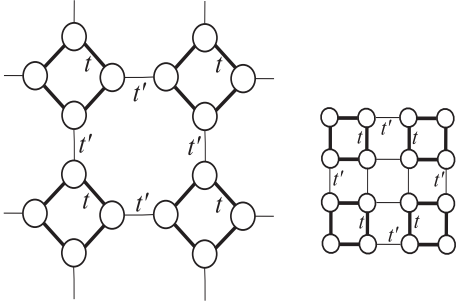


FIG. 1. The lattice considered in this paper. The inset shows the plaquette lattice in Ref. [9].

So a message of this work is that, in order to search for higher  $T_c$ 's, we should look not only at the Fermi surface but also at the atomic structure in real space.

We have used the four-band version of FLEX, [9,10,14] where the Green's function  $G$ , the spin susceptibility  $\chi$ , the self-energy  $\Sigma$ , and the superconducting gap function  $\phi$  are  $4 \times 4$  matrices, e.g.,  $G_{lm}(\mathbf{k}, i\varepsilon_n)$ , where  $l, m$  specify the four sites in a unit cell. We can go from the site indices over to band indices with a unitary transformation. For the spin susceptibility, we concentrate on its largest eigenvalue denoted as  $\chi$ . From Green's function and the spin susceptibility we obtain the superconducting gap function (with spin-singlet pairing assumed) and  $T_c$  by solving the linearized Eliashberg's equation [13]. In our analysis, we take  $32 \times 32$   $k$ -point meshes and up to 4096 Matsubara frequencies, where the numerical results are sufficiently converged. The on-site Hubbard repulsion is taken to be a typical strong-correlation value,  $U/W = 7/6$ , where  $W$  is the band width. The band filling (=number of electrons/number of sites) is taken to be a value  $n = 0.85$ , which is close, but not too close, to the half-filling where the Mott transition and antiferromagnetic order are expected. In the below we have confirmed that when the eigenvalue of Eliashberg's equation becomes unity prior to the divergence of the spin susceptibility.

The FLEX result for the spin susceptibility, Green's function, and the superconducting gap function are shown in Fig. 2 for  $t' = 0.6$  ( $t = 1.2$ ) with  $T = 0.06$ . Ridges in the Green's function delineate the Fermi surface. Fermi surface comprises two bands (second and third from the bottom), which we call band A and band

B. We can see that each band has a square-like pocket for the Fermi surface, which is reminiscent of the Fermi surface of  $\text{Sr}_2\text{RuO}_4$ , with a good reason as we shall see. On the other hand we notice that the spin susceptibility has broad peaks around  $(\pi, \pi)$ . Quite unexpectedly, the gap function has a strange structure in such a way that its amplitude on the Fermi surface is peaked at the *corners* rather than along the edges.

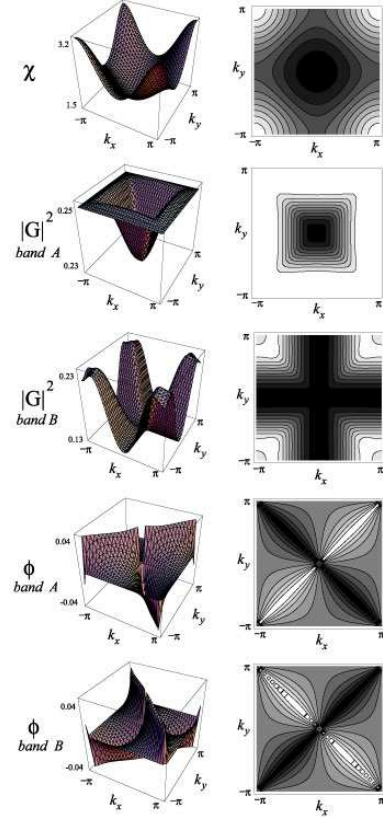


FIG. 2. Spin susceptibility ( $\chi$ ), the absolute value of the Green's function squared ( $|G|^2$ ), and the superconducting gap function  $\Phi$  against  $k_x, k_y$  for the lowest Matsubara frequency for  $U = 7$ ,  $n = 0.85$ ,  $t = 1.2$ ,  $t' = 0.6$ , and  $T = 0.06$ .

Figure 3 shows  $T_c$  as a function of  $t$ . [15] A plaquette lattice is characterized by the intra-plaquette transfer  $t$  and inter-plaquette one  $t'$ . To facilitate comparison, we have fixed the single-particle bandwidth  $W = 2(2|t| + |t'|)$  to 6, which is the value of  $W$  when  $t = t' = 1$ . Interestingly,  $T_c$  is larger for smaller  $|t'|$ , which is in accord with our expectation that the case of plaquette lattice (tetramerization in the present case) is favorable.  $T_c$  saturates to a value  $T_c = 0.06 = 0.01W$ , which is two times greater than that ( $< 0.03t$ ) for the square lattice.

The enhancement of  $T_c$  in smaller  $|t'|$  can be understood by the nesting between the disconnected Fermi surface (Fig. 4). At half filling ( $n = 1$ ) the Fermi surface is perfectly nested regardless of the value of  $|t'|$ . When less than half-filled, the nesting in the band depicted by  $Q$  in

Fig. 3 degrades but not so much for smaller  $|t'|$ . Because the effective attraction here is mediated by the antiferromagnetic spin fluctuation (with a large  $|Q|$ ),  $T_c$  is larger for better nesting, i.e., for smaller  $|t'| \propto$  the warping of the quasi-1D Fermi surface. This  $t'$ -dependence of  $T_c$  can be understood also in real space, where the intra-cell spin singlet should be more robustly formed for smaller  $|t'|$ .

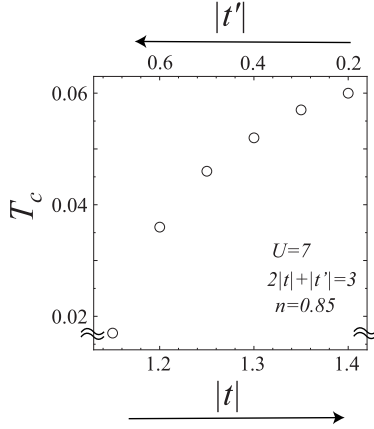


FIG. 3.  $T_c$  plotted as a function of  $t$  for  $U = 7$  and  $n = 0.85$  in units where the band width  $2(2t + t') = 6$ .

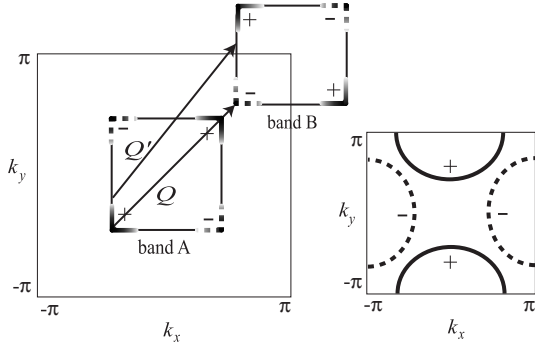


FIG. 4. Fermi surfaces of the lattice depicted in Fig.1. The solid (dashed) curves represent positive (negative) values of the gap function on the Fermi surface. The arrows represent typical momentum transfer in pair scattering processes, where  $Q$  corresponds to the wave vector at which the spin susceptibility is peaked. The solid (dashed) curves in the inset represents the positive (negative) values of the gap function in a plaquette lattice in Ref. [9].

We can explain the structures of the strange gap function in terms of molecular orbitals (Fig. 5a) and the pairing (Fig. 5b) in real space. As mentioned, the Fermi surface reminds us of the ( $\alpha$  and  $\beta$ ) bands in SrRuO<sub>3</sub>, which consists of two sets of quasi-1D array of orbitals. In the present case the quasi-1D band structure arises from the molecular orbitals in the plaquette. The molec-

ular orbitals that are relevant to bands A and B have  $p_x$ - and  $p_y$ - symmetries (Fig. 5a), so that we do have two sets of 1D arrays of orbitals. Due to the hybridization of the two orbitals, the two sets of quasi-1D Fermi surface (two, orthogonal sets of parallel lines) anticross, and we end up with two square-shaped pockets.

Now the interesting point is, the Cooper pair, arising from antiferromagnetic fluctuations, is formed across the adjacent sites (ellipses in Fig. 5b), that is *across* the two molecular orbitals. This implies that the gap function on the Fermi surface is large only around the positions at which the two ( $p_x$  and  $p_y$ ) bands hybridize, i.e., around the anticrossing points. The pairings depicted in Fig. 5b as solid ellipses and dashed ellipses have opposite signs, so that the symmetry is  $d_{xy}$ . We have thus a curious case of an inter-band pairing (a pairing formed by inter-band pair scatterings). We can in fact confirm that the pairing is interband and  $d_{xy}$  by looking at the sign of the gap function. The ellipses in Fig. 5 are represented by  $\langle C_{A(B)\uparrow} C_{A(B)\downarrow} \rangle$ , where  $C_{A(B)\sigma} \equiv C_{1\sigma} - C_{2(4)\sigma} + C_{4(2)\sigma} - C_{3\sigma}$ , where  $C_{i\sigma}$  annihilates an electron with spin  $\sigma$  at site  $i$  as numbered in Fig.5. When the pairing is formed across adjacent sites we can show  $\langle C_{A\uparrow} C_{A\downarrow} \rangle = -\langle C_{B\uparrow} C_{B\downarrow} \rangle$  (opposite signs across the bands) with an odd parity ( $d_{xy}$ ) against  $k_x \leftrightarrow -k_x$  or  $k_y \leftrightarrow -k_y$ .

This explains why the gap function changes sign within each pocket. Hence the  $s$ -wave symmetry on each pocket is not a necessary condition for a high  $T_c$ . Even when there are intra-pocket sign changes, the disconnectivity of the Fermi surface plays an important role, since the *inter-pocket* sign change associated with  $Q$  does exploit this in avoiding intersecting the Fermi surface.

One might then wonder why the intra-pocket sign changes do not reduce  $T_c$ , since the pair-scattering processes depicted by  $Q'$  in Fig. 4 connecting the  $k$ -points across which the gap function has the same sign would normally reduce  $T_c$ . In the present case, however, we have an ingenious situation where the gap function is strongly peaked at the position (corners in this example) where hybridization occurs, so that the  $Q'$  processes, being off the peak, have little effect.

How is the present model compared with the lattice considered in Ref. [9], where the plaquette is a four-membered ring in either case. Here the consideration in real space comes in handy. The latter case is a 2D system rather than quasi-1D, where the pockets arise due to a band folding due to the tetramerization. The pairing in real space is formed within each molecular orbital (Fig. 6) unlike the present case, so the superconducting gap function has an  $s$ -wave symmetry on each Fermi surface pocket (but opposite signs across the two pockets with the nesting  $Q \approx 0$  due to the band folding (inset of Fig. 4). Despite of this distinction, the resulting  $T_c$ 's are similar between the two cases.

Another interesting comparison is with  $\text{Sr}_2\text{RuO}_4$  [16,17], which also suggests an importance of the real space structure. Although the Fermi surface is quasi-1D in  $\text{Sr}_2\text{RuO}_4$  as well, the oxide has strong pieces of evidence for triplet pairing, and even when one considers the spin-singlet pairing,  $T_c$  (for the  $\alpha, \beta$  bands for this material) estimated with the FLEX is very small [17]. Due to the quasi-one dimensionality the spin susceptibility  $\chi(\mathbf{q}, \omega)$  has linear ridges in  $k$ -space. As a result, the pair scatterings have large contributions all over the ridges, so that the (extended)  $s$ -wave gap function involves unfavorable pair scatterings across which the gap has the same sign, resulting in the reduced  $T_c$ . This makes the spin-triplet,  $p$ -wave pairing more favorable, for which the resulting gap function has large amplitudes all over the Fermi surface, except for dips at the corners. By contrast, the present case has a built-in antiferromagnetic structure within the unit cell in real space, so that the spin susceptibility has a well-defined peak around  $(\pi, \pi)$ . This makes a specific  $\mathbf{Q}$  to be relevant in the pair scattering, which makes the gap function peaked at specific points, which in turn gives rise to an enhancement in  $T_c$ .

To summarize, we should question not only the structure of the Fermi surface but also the structure of the molecular orbitals and the superconducting pairings in real space in understanding the superconductivity from the electron repulsion. One interesting tendency is that high  $T_c$ 's are found in plaquette systems where unit cells having multiple sites are connected with a relatively small inter-plaquette hopping [8–10], which also suggests the importance of the real space picture. In fact, the relation between real-space and the momentum-space pictures has been discussed for systems consisting of dimers recently. [10] It is an interesting future problem to see how the real-space and the momentum-space pictures are related with each other for wider class of systems in realizing high  $T_c$ 's.

We wish to thank Professor J. Akimitsu for valuable discussions. This work was supported in part by a Grant-in-Aid for Scientific Research and Special Coordination Funds from the Ministry of Education of Japan. Numerical calculations were performed at the Supercomputer Center, Institute for Solid State Physics, University of Tokyo.

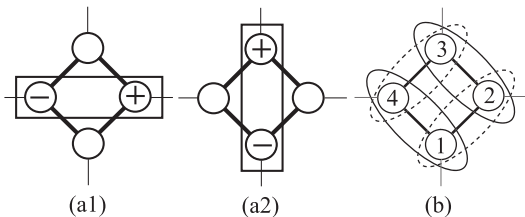


FIG. 5. (a) Intra-plaquette molecular orbitals with  $p_x$  (a1) and  $p_y$  (a2) symmetries. (b) Cooper pairs with solid and dashed ellipses indicating pairing amplitudes with opposite signs.

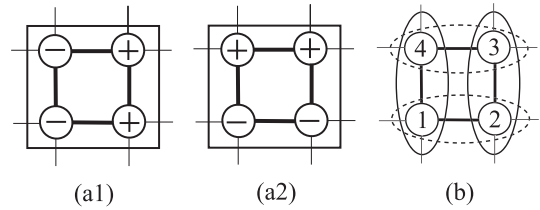


FIG. 6. (a) Intra-plaquette molecular orbitals with  $p_x$  (a1) and  $p_y$  (a2) symmetries, and (b) Cooper pairs for the lattice considered in Ref. [9].

- 
- [1] J.G. Bednorz and K.A. Müller, Z. Phys. B **64**, 189 (1986).
  - [2] N.E. Bickers, D.J. Scalapino, and S.R. White, Phys. Rev. Lett. **62**, 961 (1989).
  - [3] S. Grabowski, M. Langer, J. Schmalian, and K.H. Bennemann, Europhys. Lett. **34**, 219 (1996).
  - [4] T. Dahm and L. Tewordt, Phys. Rev. B **52**, 1297 (1995).
  - [5] See, e.g., D.J. Scalapino, E. Loh, and J.E. Hirsch, Phys. Rev. B **35**, 6694 (1987); S.R. White, D.J. Scalapino, R.L. Sugar, N.E. Bickers, and R.T. Scalettar, Phys. Rev. B **39**, 839 (1989).
  - [6] K. Kuroki and H. Aoki, Phys. Rev. B **56**, R14287 (1997).
  - [7] R. Arita, K. Kuroki, and H. Aoki, J. Phys. Soc. Jpn. **69**, 1181 (2000).
  - [8] K. Kuroki and R. Arita, Phys. Rev. B **64**, 024501 (2001).
  - [9] T. Kimura, H. Tamura, K. Kuroki, K. Shiraishi, H. Takayanagi, and R. Arita, unpublished (cond-mat/0204218).
  - [10] K. Kuroki, T. Kimura, and R. Arita, unpublished (cond-mat/0206204).
  - [11] K. Kuroki and R. Arita, Phys. Rev. B **63**, 174507 (2001).
  - [12] B. Albert and K. Schmitt, Inorg. Chem. **38**, 6159 (1999).
  - [13] G.M. Eliashberg, Zh. Eksp. Teor. Fiz. **38**, 996 (1960) [Soviet Phys. JETP **11**, 696 (1960)].
  - [14] K. Kuroki, T. Kimura, R. Arita, Y. Tanaka, and Y. Matsuda, Phys. Rev. B **65**, 100516 (2002).
  - [15]  $T_c$  depends only on the absolute values of  $t$  or  $t'$ . The invariance under  $t \rightarrow -t$  and/or  $t' \rightarrow -t'$  can be shown with a gauge transformation,  $C_{1(3)} \rightarrow -C_{1(3)}$  and  $C_{2(4)} \rightarrow -C_{2(4)}$  for  $t \rightarrow -t$ , and  $C_n \rightarrow (-1)^{x+y} C_n$  ( $n = 1, 2, 3, 4$ ) for  $t' \rightarrow -t'$ , where  $x$  and  $y$  are the position of the unit cell measured in units of the cell size.
  - [16] Y. Maeno, H. Hashimoto, K. Yoshida, S. Nishizaki, T. Fujita, J.G. Bednorz, and F. Lichtenberg, Nature (London) **372**, 532 (1994).
  - [17] K. Kuroki, M. Ogata, R. Arita, and H. Aoki, Phys. Rev. B **63**, 060506(R) (2001).